Lkb1 regulates organogenesis and early oncogenesis along AMPK-dependent and -independent pathways

Bryan Lo, Geraldine Strasser, Meredith Sagolla, Cary D. Austin, Melissa Junttila, and Ira Mellman

Genentech, South San Francisco, CA 94080

The tumor suppressor Lkb1/STK11/Par-4 is a key regulator of cellular energy, proliferation, and polarity, yet its mechanisms of action remain poorly defined. We generated mice harboring a mutant Lkb1 knockin allele that allows for rapid inhibition of Lkb1 kinase. Culturing embryonic tissues, we show that acute loss of kinase activity perturbs epithelial morphogenesis without affecting cell polarity. In pancreas, cystic structures developed rapidly after Lkb1 inhibition. In lung, inhibition resulted in cell-autonomous branching defects. Although the lung phenotype was rescued by an activator of the Lkb1 target adenosine monophosphate–activated kinase (AMPK), pancreatic cyst development was independent of AMPK signaling. Remarkably, the pancreatic phenotype evolved to resemble precancerous lesions, demonstrating that loss of Lkb1 was sufficient to drive the initial steps of carcinogenesis ex vivo. A similar phenotype was induced by expression of mutant K-Ras with p16/p19 deletion. Combining culture of embryonic tissues with genetic manipulation and chemical genetics thus provides a powerful approach to unraveling developmental programs and understanding cancer initiation.

Introduction

Germline mutations in the serine/threonine kinase Lkb1 (Par-4/STK11/XEEK1) result in Peutz-Jeghers syndrome (PJS), an autosomal-dominant syndrome characterized by benign gastrointestinal hamartomas and pigmentation abnormalities (Jeghers et al., 1949; Hemminki et al., 1998; Jenne et al., 1998). PJS patients are at increased risk for developing epithelial cancers (Hearle et al., 2006; Mehenni et al., 2006) with most PJS alleles reflecting deletions or inactivating mutations in the kinase domain of Lkb1 (Alessi et al., 2006). In addition, many sporadic cancers exhibit Lkb1 mutations or deletion, especially adenocarcinoma of the lung (at least 30% of cases; Sanchez-Cespedes, 2007).

Lkb1 (Par-4) is of additional interest because of its role in controlling asymmetric partitioning of the *Caenorhabditis elegans* embryo (Kemphues et al., 1988). It also has been implicated as a key regulator of cell polarity in cultured epithelial cells (Baas et al., 2004). How Lkb1 accomplishes these and its other diverse functions, however, is poorly understood. Lkb1 is best known for its ability to phosphorylate and activate AMP kinase (AMPK) as part of a sensing mechanism of cellular energy status with inputs into metabolic pathways and mTOR activity (Hawley et al., 2003; Lizcano et al., 2004; Shaw et al., 2004). Although these two components themselves have been linked to a variety of additional functions such as adhesion, proliferation, and polarity, Lkb1 likely has several additional relevant targets (Baas et al., 2004; Lee et al., 2007; Mirouse et al., 2007; ten Klooster et al., 2009). For example, Par-1 is the Lkb1 target in the *C. elegans* embryo that contributes to defining its posterior domain (Kemphues et al., 1988), and MARK2, the Par-1 mammalian homologue, is targeted by an *Helicobacter pylori* virulence factor to disrupt epithelial polarity (Saadat et al., 2007). The SAD-A/B kinases and SIK1/2 kinases together with Lkb1 modulate neuronal polarization (Barnes et al., 2007) and anoikis (Cheng et al., 2009), and Lkb1-NUAK signaling controls a phosphatase complex that regulates myosin light chain and cell adhesion (Zagórska et al., 2010).

Genetic evidence from mouse models has clearly demonstrated that Lkb1 is a tumor suppressor, although it is unclear which of its activities are most relevant, if these activities are

B. Lo and G. Strasser contributed equally to this paper.

Correspondence to Ira Mellman: mellman.ira@gene.com

Abbreviations used in this paper: AAV, adeno-associated virus; AMPK, AMP-activated kinase; ASKA, analogue-sensitive kinase allele; DIV, days in vitro; E, embryonic day; EdU, 5-ethynyl-2-deoxyuridine; MEF, mouse embryonic fibroblast; PanIN, pancreatic intraepithelial neoplasia; PJS, Peutz-Jeghers syndrome.

The Rockefeller University Press $30.00
J. Cell Biol. Vol. 199 No. 7 1117–1130
www.jcb.org/cgi/doi/10.1083/jcb.201208080

the same in cancers of different tissues, or even if Lkb1's kinase activity is required. Although Lkb1$^{-/-}$ mice die early in embryogenesis (Ylikorkala et al., 2001; Jishage et al., 2002), heterozygous littermates develop gastrointestinal hamartomas (Bardeesy et al., 2002; Miyoshi et al., 2002; Rossi et al., 2002). Conditional deletions of Lkb1 result in metaplasias and neoplasias (Hezel et al., 2008; Pearson et al., 2008; Shorning et al., 2009), whereas loss of Lkb1 combined with an activated oncogene or inactivation of a second mutant tumor suppressor provokes more rapid tumor development in lung, pancreas, and various other organs (Ji et al., 2007; Huang et al., 2008; Morton et al., 2010).

Although Cre-mediated inactivation of Lkb1 has established the importance of Lkb1 in normal development and oncogenesis in a variety of mammalian organ systems, progress has been greatly limited by the fact that such models have not enabled mechanistic analysis. Knockouts provide only chronic inactivation of Lkb1 in a fashion that cannot be manipulated either spatially or temporally. In addition, the effects obtained by gene deletions may not reproduce phenotypes associated with kinase inactivation because the nonkinase domains of Lkb1 could serve as a scaffold for other proteins. Thus, there is a clear need to complement standard gene inactivation approaches with strategies that allow for specific, acute, and reversible inhibition of Lkb1 kinase activity and under conditions where these effects can be monitored in living cells. To this end, we have produced a mouse expressing an analogue-sensitive kinase allele (ASKA) of Lkb1 that can be inhibited by membrane-permeable derivatives of the small molecule inhibitor PP1 (Bishop et al., 2000). By combining with a generally applicable approach to ex vivo culture of developing embryonic organs, we have found that Lkb1 kinase activity functions differently in the morphogenesis of different epithelial tissues. Moreover, our experimental system can be used to generate what appear to be the earliest events in tumor formation, enabling detailed cell biological, biochemical, and genetic analysis.

Results

Lkb1 does not control intrinsic epithelial cell polarity in MDCK cells

The observation that activation of functional Lkb1 in a colon cancer cell line rapidly induced polarity (Baas et al., 2004) led us to investigate whether loss of Lkb1 in a nontransformed epithelial cell would result in disruption of polarity. Endogenous Lkb1 was stably knocked down using shRNA in MDCK cells (Fig. 1 A, left), but, surprisingly, Lkb1 loss did not perturb apical-basal polarity. In MDCK monolayers (Fig. 1 A, middle) and in spheroids grown as 3D Matrigel cultures (Fig. 1 A, right), the pattern of apical, basolateral, and tight junctional markers remained unchanged. Although loss of Lkb1 did result in a delay in calcium-induced tight junction assembly (unpublished data), a subtle polarity-related phenotype previously seen in MDCK cells overexpressing dominant-negative Lkb1 or AMPK alleles (Zhang et al., 2006; Zheng and Cantley, 2007), lack of a strong apical-basal polarity phenotype suggested to us that Lkb1 does not control intrinsic cell polarity in MDCK cells. Nevertheless, rapid adaptation to Lkb1 knockdown or the lack of a tissue context may have obscured a role for Lkb1 in regulating polarity. We therefore developed a mouse model using a chemical-genetic approach that allows for acute and reversible inhibition of Lkb1 kinase activity in a physiological context.

Generation of Lkb1 ASKA knockin mice

For a range of kinases, mutation of the "gatekeeper" residue in the ATP-binding pocket renders the kinase susceptible to small molecule analogues of the general kinase inhibitor PP1 (Bishop et al., 2000). We identified the methionine at position 129 as the gatekeeper residue for Lkb1 by analysis of the primary amino acid sequence (Zhang et al., 2005) and substituted a glycine to create Lkb1^{M129G} (Fig. S1 A). Using HeLa cells, we first verified that Lkb1^{M129G} retained kinase activity toward its substrate AMPK and that this activity was inhibited by 1NMPP1 (Fig. S1 B). We then generated knockin mice to replace the wild-type Lkb1 with Lkb1^{M129G} (Fig. 1 B; see Materials and methods).

Results of heterozygous intercrosses indicated that mice homozygous for Lkb1^{M129G} (hereafter referred to as Lkb1^{MG}) exhibited an unexpected late embryonic lethality. Histological examination of embryonic day (E) 14.5 embryos, however, uncovered no significant differences in the developmental patterning of Lkb1$^{MG/MG}$ embryos compared with wild-type littermates, indicating gastrulation and organogenesis were unaffected by the knockin allele (Fig. 1 C). This was in sharp contrast to the early (E9.5) embryonic lethality with vascular and severe neural tube defects seen in Lkb1 null mice (Ylikorkala et al., 2001; Jishage et al., 2002). Because no anatomical abnormality was identified, we speculated that Lkb1^{MG} is a hypomorphic allele that caused placental or metabolic insufficiency late in gestation.

Indeed, in mouse embryonic fibroblasts (MEFs), the steady-state levels of Lkb1^{MG} protein were significantly reduced relative to the wild-type protein (Fig. 1 D, lanes 1 and 2 vs. 5 and 6). The reduction likely reflected posttranslational protein instability because RT-PCR showed no reduction in Lkb1^{MG} mRNA levels (Fig. S1 C). Moreover, the addition of 1NMPP1 increased Lkb1^{MG} protein levels (Fig. 1 D, lanes 7 and 8; and Fig. S1 D), suggesting that binding of the ATP analogue stabilized the mutant kinase in a conformation less susceptible to degradation. Nevertheless, Lkb1^{MG} retained the ability to phosphorylate and activate its substrate AMPK despite reduced protein levels, and this activity was effectively inhibited by 1NMPP1 (Fig. 1 D, lane 6 vs. 8).

Chemical genetics applied to embryonic explants

Although unable to generate a homozygous Lkb1^{MG} mouse strain, we were able to study Lkb1 function under conditions that permitted more detailed cell biological analysis than is possible in vivo. We modified existing approaches to culturing embryonic organs to enable high resolution imaging, pharmacologic manipulation, and biochemical analysis ex vivo. We focused on lung and pancreas, organs that give rise to cancers where Lkb1 loss is relatively common (Sahin et al., 2003; Sanchez-Cespedes, 2007).

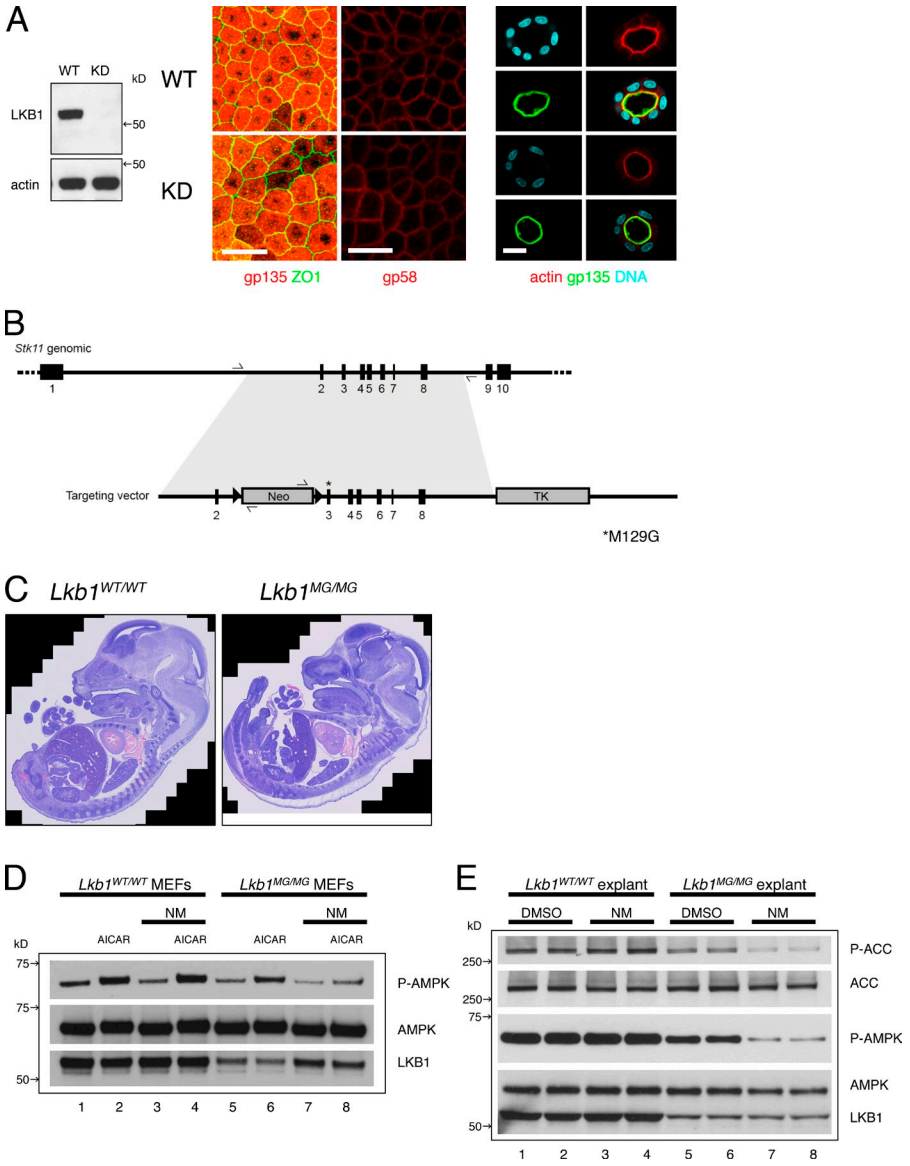

Figure 1. **Development of an Lkb1 ASKA knockin mouse.** (A, left) Lkb1 was stably knocked down in MDCK cells using a retroviral shRNA system. Cell lysates were blotted with antibodies to Lkb1 and actin. (middle) The tight junction marker ZO-1, apical marker gp135, and basolateral marker gp58 are properly localized in control (WT) and Lkb1 knockdown (KD) cells grown as monolayers. (right) The cortical actin network and apical marker gp135 are also properly localized in MDCK spheroids when the cells were grown in 3D Matrigel cultures. Bars, 20 µm. (B) A targeting vector was generated carrying the M129G mutation in exon 3 of *Stk11* genomic DNA and a neomycin cassette flanked by two LoxP sites. The final targeted allele contained the M129G mutation and an adjacent intron with a single LoxP site. (C) Hematoxylin-eosin–stained sections of E14.5 $Lkb1^{WT/WT}$ (left) and $Lkb1^{MG/MG}$ (right) littermate embryos showing intact organogenesis. (D) $Lkb1^{MG}$ protein levels are stabilized and kinase activity is inhibited by 1NMPP1 in MEFs. MEFs from $Lkb1^{WT/WT}$ (lanes 1–4) and $Lkb1^{MG/MG}$ (lanes 5–8) embryos were incubated for 16 h with DMSO (lanes 1, 2, 5, and 6) or 1 µM 1NMPP1 (lanes 3, 4, 7, and 8), and then treated with or without 2 mM AICAR for 1 h before collecting cell lysates. Western blots were analyzed with antibodies to Phospo-AMPKα (Thr172), AMPKα, and Lkb1. (E) $Lkb1^{MG}$ kinase activity in embryonic explants is inhibited by 1NMPP1. Duplicate embryonic explants (pancreas; see Fig. 3) from $Lkb1^{WT/WT}$ (lanes 1–4) and $Lkb1^{MG/MG}$ (lanes 5–8) embryos were cultured in vitro on transwell filters and incubated 2 h with DMSO (lanes 1, 2, 5, and 6) or 1 µM 1NMPP1 (lanes 3, 4, 7, and 8) before collecting lysates. Western blots were analyzed with antibodies to Phospho-ACC(Ser79), ACC, Phospo-AMPKα(Thr172), AMPKα, and Lkb1.

Tissues were harvested from $Lkb1^{WT/WT}$ and $Lkb1^{MG/MG}$ littermate embryos and explants were cultured at the air–media interface on polyester filters with either vehicle control (DMSO) or inhibitor (1NMPP1). Addition of 1 µM 1NMPP1 for 2 h led to an acute reduction in phospho-T172 AMPK in $Lkb1^{MG/MG}$ explant pancreata (Fig. 1 E, lanes 5–8), whereas no such reduction was observed for $Lkb1^{WT/WT}$ explants (Fig. 1 E, lanes 1–4). The reduction in phospho-T172 levels reflected an actual reduction in AMPK activity given the concomitant decrease in phosphorylation of the AMPK target acetyl-CoA carboxylase (ACC; Fig. 1 E). As had been observed in the MEFs, reduced steady-state levels of $Lkb1^{MG}$ protein were also seen in the explant lysates, and incubations (>16 h) with 1NMPP1 led to stabilization of $Lkb1^{MG}$ (unpublished data).

Inhibition of Lkb1 kinase activity results in branching defects in embryonic lung

Whole lung organ cultures from $Lkb1^{WT/WT}$ embryos at E12.5 continued to grow and undergo highly stereotypic branching morphogenesis (Metzger et al., 2008) in a fashion that was unaffected by the presence of 1NMPP1 (Fig. 2 A, top). $Lkb1^{MG/MG}$ lung explants also continued to grow in the presence of inhibitor; however, they displayed defects in branching and bud septation, resulting in significantly increased terminal bud width and smaller overall size by 1–2 d in vitro (DIV; Fig. 2 A, bottom; and see Fig. S5 A for quantitation of bud widths).

To determine if alterations in morphogenesis reflected an underlying disruption of epithelial cell polarity, we fixed and stained lung explants with several apical, basal, and junctional markers. Confocal microscopy of explants showed that regardless of genotype or drug treatment, lung epithelia showed normal distributions of E-cadherin and Mucin1 (Muc-1) (Fig. 2 B). Additionally, apical distribution of aPKC, tight junction marker ZO-1, and basolateral distribution of β-catenin were unchanged after Lkb1 inhibition (unpublished data). Thus, inhibition of Lkb1 kinase activity resulted in defective lung branching morphogenesis without a significant disruption in epithelial apical-basal polarity.

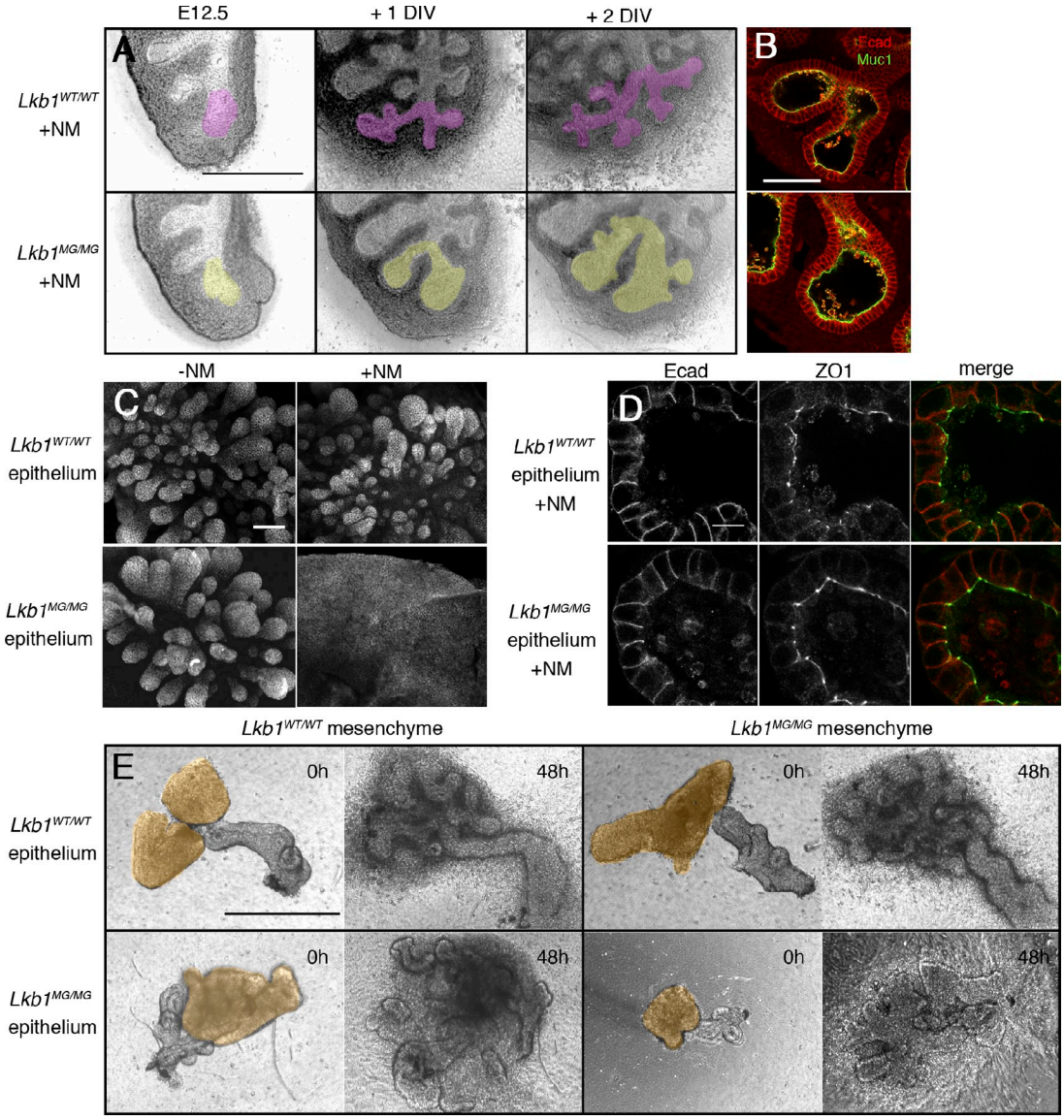

Figure 2. **Inhibition of Lkb1 in the lung results in abnormal branching but not polarity defects.** (A) E12.5 lung explants were cultured on transwell filters for 2 DIV with 1 µM 1NMPP1. Branches derived from a single bud are pseudocolored. (B) 1NMPP1-treated Lkb1$^{WT/WT}$ (top) and Lkb1$^{MG/MG}$ (bottom) epithelial buds show similar patterns of E-cadherin and Muc-1 staining. (C) Mesenchyme-free epithelial explants grown in matrigel show branching defects when Lkb1 activity is inhibited. (D) E-cadherin and ZO-1 staining patterns are similar between Lkb1$^{WT/WT}$ (top) and Lkb1$^{MG/MG}$ (bottom) mesenchyme-free epithelial explants, both grown in the presence of 1NMPP1. (E) Branching phenotype of epithelial tissue co-cultured with mesenchyme in transplant experiments depends on the genotype of the epithelium but not the mesenchyme. The four combinations of epithelial-mesenchymal co-cultures grown in the presence of 1NMPP1 are shown at setup (with mesenchyme pseudocolored) and at 48 h. Bars: (A and E) 500 µm; (B and C) 100 µm; (D) 10 µm.

Because conditional Cre-mediated deletions of Lkb1 in the intestine have suggested roles for Lkb1 signaling in both epithelial and mesenchymal cells (Katajisto et al., 2008), we next asked if the defect in branching morphogenesis was epithelial cell autonomous. Portions of lung epithelia were stripped of mesenchyme and embedded in Matrigel (Nogawa and Ito, 1995). In the presence and absence of 1NMPP1, isolated E12.5 Lkb1$^{WT/WT}$ epithelium displayed extensive growth and budding in response to exogenous growth factors such as FGF1 or FGF7 (Fig. 2 C, top). Isolated E12.5 Lkb1$^{MG/MG}$ epithelium cultured in the presence of 1NMPP1, however, generated large sacs and flat sheets of epithelium (Fig. 2 C, bottom), consistent with the defective branching seen in Lkb1-inhibited whole lung explants. Again, localization of apical and basal polarity markers was unaffected (Fig. 2 D). The effect of Lkb1 kinase inhibition on lung morphogenesis was consistent with an epithelial cell-autonomous phenotype.

The mesenchyme-free isolated epithelium experiments required the addition of exogenous growth factors that are normally supplied by the mesenchyme (Cardoso et al., 1997), raising the possibility that mesenchymally derived signals may be defective. To assess this possibility, epithelium/mesenchyme complementation experiments were performed. Explants of distal epithelium from Lkb1$^{WT/WT}$ or Lkb1$^{MG/MG}$ lungs were isolated and transferred to Matrigel. A reserved portion of distal Lkb1$^{WT/WT}$ or Lkb1$^{MG/MG}$ mesenchymal tissue was then positioned in direct

contact with the epithelium, and the co-cultures were fed with media containing 1NMPP1. In the absence of added growth factors, both Lkb1$^{MG/MG}$ and Lkb1$^{WT/WT}$ mesenchyme were equally effective in supporting normal growth and branch development in Lkb1$^{WT/WT}$ epithelium (Fig. 2 E). Conversely, Lkb1$^{WT/WT}$ mesenchyme failed to restore normal development to Lkb1$^{MG/MG}$ epithelium in the presence of 1NMPP1. The fact that the branching phenotype always reflected the genotype of the epithelium provided strong evidence that Lkb1 controlled lung morphogenesis in an epithelial cell-autonomous fashion.

Inhibition of Lkb1 kinase activity results in cyst formation in late but not early stage pancreas explants

The pancreas, like the lung, undergoes branching morphogenesis during development. However, its developmental program is less stereotyped and involves the formation of a multi-lumen plexus that coordinately extends and remodels into a single lumen ductal system (Villasenor et al., 2010). We followed the growth and branching of E12.5 embryonic pancreata from Lkb1$^{WT/WT}$ and Lkb1$^{MG/MG}$ mice harboring a Pdx1-GFP reporter (Holland et al., 2006; Puri and Hebrok, 2007) to highlight the developing pancreatic endoderm (Fig. 3 A). After growth in the presence or absence of 1NMPP1, we fixed and stained explants with epithelial markers to examine the pattern of branching with confocal microscopy (Fig. 3 B). Lkb1 inhibition did not markedly perturb the pattern of growth or branching morphogenesis (in contrast to the lung) or the polarity of individual epithelial cells in these early stage pancreata, even after culturing for 3 DIV.

In pancreata harvested from later stage embryos (E16.5), however, inhibition of Lkb1 kinase activity resulted in a dramatic alteration in tissue architecture. Lkb1$^{WT/WT}$ and Lkb1$^{MG/MG}$ explants from E16.5 littermate embryos were treated with 1 µM 1NMPP1 for 3 d. As shown in Fig. 3 C (left), phase-contrast microscopy revealed that clusters of developing acinar structures in the Lkb1$^{WT/WT}$ explant had been largely replaced by multiple cyst-like structures in the Lkb1$^{MG/MG}$ explant. Hematoxylin-eosin–stained sections indicated the cysts were lined by a monolayer of epithelial cells (Fig. 3 C, middle) and fluorescence images of pancreata expressing Pdx1-GFP confirmed that these cells expressed Pdx1, a marker of the pancreatic endoderm (Fig. 3 C, right). These results showed that inhibition of Lkb1 in late stage pancreata results in a neoplasia where acinar structures are replaced by endodermally derived cystic structures.

Cysts induced by Lkb1 inhibition resembled pancreatic cystic neoplasias that develop in a Pdx1-Cre–driven Lkb1 deletion mouse model in which modest apical-basal polarity defects were reported in the pancreatic epithelium in vivo (Hezel et al., 2008). However, in whole-mount E16.5 Lkb1$^{MG/MG}$ explants treated with 1NMPP1, no alterations in the distribution of ZO-1, E-cadherin, or Muc-1 were detected as compared with wild-type tissues (Fig. 3 D). In particular, in regions exhibiting cyst formation, E-cadherin staining was normal and the pattern of ZO-1 outlined a morphologically continuous network of tight junctions (Fig. 3 E). The high resolution immunofluorescence imaging made possible by whole-mount preparations demonstrated that although Lkb1 inhibition results in dramatic cyst formation in late stage pancreata, the neoplasias were not associated with alterations in apical-basal polarity.

Pancreatic cysts are dynamic

The rapid rate of cyst formation suggested that the cysts might be dynamic structures. Epithelial cells lining the cysts showed enlargement of the apical domain and a flattened morphology suggestive of tension derived from fluid accumulation. Fluorescence time-lapse microscopy of live Lkb1$^{MG/MG}$ pancreata cultured from Pdx1-GFP transgenic embryos treated with 1NMPP1 demonstrated that cyst formation was a highly dynamic biphasic process. In the first phase (24–48 h after addition of 1NMPP1), cysts typically exhibited several cycles of rapid growth and contraction, suggesting that fluid shifts were highly dynamic rather than a gradual and steady accumulation of fluid (Video 1). In the second phase (48–72 h), cysts that reached some threshold size either continued to grow slowly or to stabilize, suggesting an equilibrium had been reached. Importantly, this cystic phenotype was never observed in explants from wild-type mice treated with 1NMPP1 (see Table S3 for quantification of cystic phenotype).

To assess the cellular basis for these dynamic changes, we collected confocal z-stacks every 8–12 h after Lkb1 inhibition. As shown in Fig. 4 A, cysts arising in the distal ductal compartment connected clusters of differentiating acinar structures (white arrows). At early time points cysts were small and the acinar structures remained largely intact. This suggested that during cyst initiation acinar to ductal transdifferentiation plays a relatively minor role in contrast to what has been inferred from static images examined by conventional histology (Hezel et al., 2008). Only when the cysts fully enlarged did cells that originally comprised acinar structures become incorporated into the wall of an adjacent cyst (Fig. 4 A, yellow arrows). The eventual loss of acinar structures thus appeared largely to be caused by these incorporation events as opposed to death or de-differentiation of developing acinar cells because activated caspase-3 staining and sytox fluorescence imaging did not show increased cell death in 1NMPP1-treated Lkb1$^{MG/MG}$ explants (Fig. S2).

Increased epithelial cell proliferation also accompanies the growth of pancreatic cysts

Given that Lkb1 has been shown to be a negative regulator of cell cycle entry (Zeng and Berger, 2006), we asked if increased cellular proliferation might contribute to enlargement of pancreatic cysts. In 1NMPP1-treated E16.5 Lkb1$^{MG/MG}$ explants, 5-ethynyl-2-deoxyuridine (EdU) labeling showed that a higher proportion of the epithelial cells lining cysts were actively proliferating relative to controls (Fig. 4 B). Using flow cytometry analysis of E16.5 Lkb1$^{WT/WT}$ and Lkb1$^{MG/MG}$ explants treated with 1NMPP1 for 3 d and then incubated with a 2-h pulse of EdU, EpCAM-positive cells from the Lkb1$^{MG/MG}$ explants were found to exhibit a significant increase in the EdU-positive population (Fig. 4 C, Fig. S5 B, and Table S1). Notably, experiments with heterozygous Lkb1$^{WT/MG}$ explants treated with 1NMPP1 did not show an increase in EdU incorporation, suggesting haploinsufficiency of Lkb1 was not sufficient for the effect on proliferation.

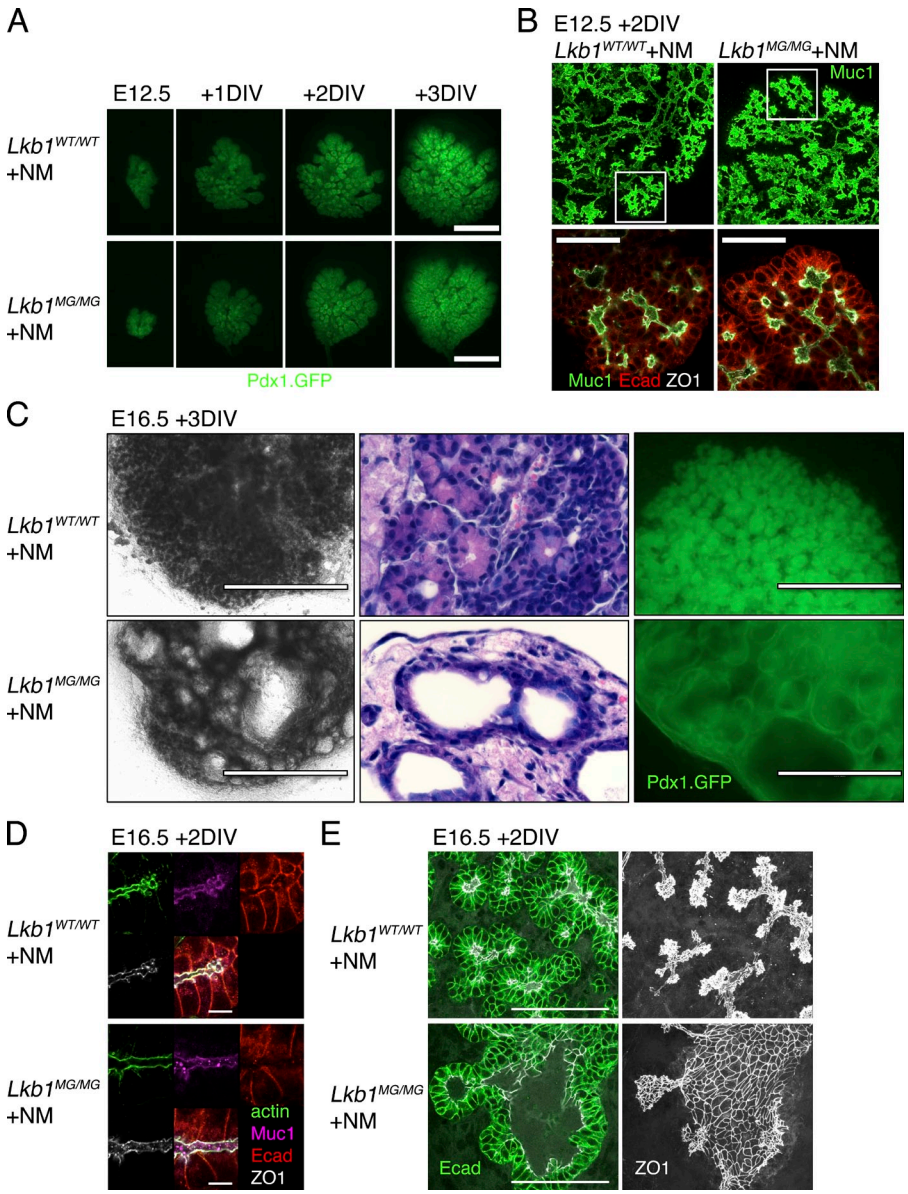

Figure 3. **Inhibition of Lkb1 results in pancreatic cystic neoplasias but not polarity defects.** (A) Lkb1$^{WT/WT}$ (top) and Lkb1$^{MG/MG}$ (bottom) E12.5 pancreatic explants were cultured on transwell filters for 3 DIV with 1 µM 1NMPP1. General pattern of growth and branching is visualized using Pdx1-GFP. (B) 1NMPP1-treated Lkb1$^{WT/WT}$ (top) and Lkb1$^{MG/MG}$ (bottom) E12.5 pancreatic explants show similar patterns of Muc-1, E-cadherin, and ZO-1 staining. (C) Lkb1$^{WT/WT}$ (top) and Lkb1$^{MG/MG}$ (bottom) E16.5 pancreatic explants were cultured with 1 µM 1NMPP1 for 3 d. Lkb1$^{MG/MG}$ explants develop multiple fluid-filled cysts lined by Pdx1-expressing epithelial cells. Phase microscopy (left), hematoxylin-eosin stained sections (middle), and fluorescence microscopy of Pdx1-GFP–expressing explants (right). (D) 1NMPP1-treated Lkb1$^{WT/WT}$ (top) and Lkb1$^{MG/MG}$ (bottom) E16.5 pancreatic explants show similar patterns of Muc-1, E-cadherin, ZO-1, and actin staining. (E) E-cadherin and ZO-1 pattern of staining in a developing cyst (note: ZO-1 pattern is a projection across a 10-µm z-stack). Bars: (A) 500 µm; (B) 50 µm; (C) 1,000 µm (phase), 400 µm (fluorescence); (D) 10 µm; (E) 100 µm.

Lung morphogenesis defects depend on AMPK, whereas pancreatic cyst formation occurs independently of AMPK

Although it is well established that Lkb1 phosphorylates and activates AMPK, Lkb1 can phosphorylate other targets (Lizcano et al., 2004). Moreover, the Thr172 in the activation loop of AMPK phosphorylated by LKB1 can also be acted on by other kinases such as CaMKK and TAK1. Therefore, the finding that 1NMPP1 treatment decreased AMPK phosphorylation in Lkb1$^{MG/MG}$ explants (Fig. 1 E) did not necessarily implicate AMPK in the development of pancreatic cystic neoplasias or lung branching defects. To assess the role of the Lkb1–AMPK pathway in the embryonic explants, we used the accessibility of the ex vivo culture system in experiments using a direct allosteric activator of AMPK, A-769662 (Göransson et al., 2007; Sanders et al., 2007). If the morphogenesis defects were a result of inhibition of the Lkb1–AMPK pathway, activation of AMPK by A-769662 would bypass the inhibition of Lkb1 and suppress the formation of pancreatic cysts and lung branching defects. This approach was validated by control experiments using Lkb1$^{MG/MG}$ MEFs; the decrease in ATP levels induced by 1NMPP1-mediated inhibition of Lkb1 could be fully reversed by the addition of A-769662 (Fig. 5 A).

In lung explants, A-769662 suppressed branching defects induced by Lkb1 inhibition. Addition of A-769662 to Lkb1$^{WT/WT}$ mesenchyme-free lung explant cultures had no effect on growth or bud formation (Fig. 5 B, left), indicating that A-769662 had no significant toxic or off-target effects. When A-769662 was added to Lkb1$^{MG/MG}$ explants, however, the large sacs and flattened sheets of epithelium induced by 1NMPP1 instead developed as numerous small buds of epithelium highly reminiscent of controls (Fig. 5 B, right). The wild-type branching phenotype thus appeared to be largely rescued by A-769662 in the Lkb1$^{MG/MG}$ explants, suggesting that Lkb1 signaling via AMPK controls morphogenesis in the lung (Table S2).

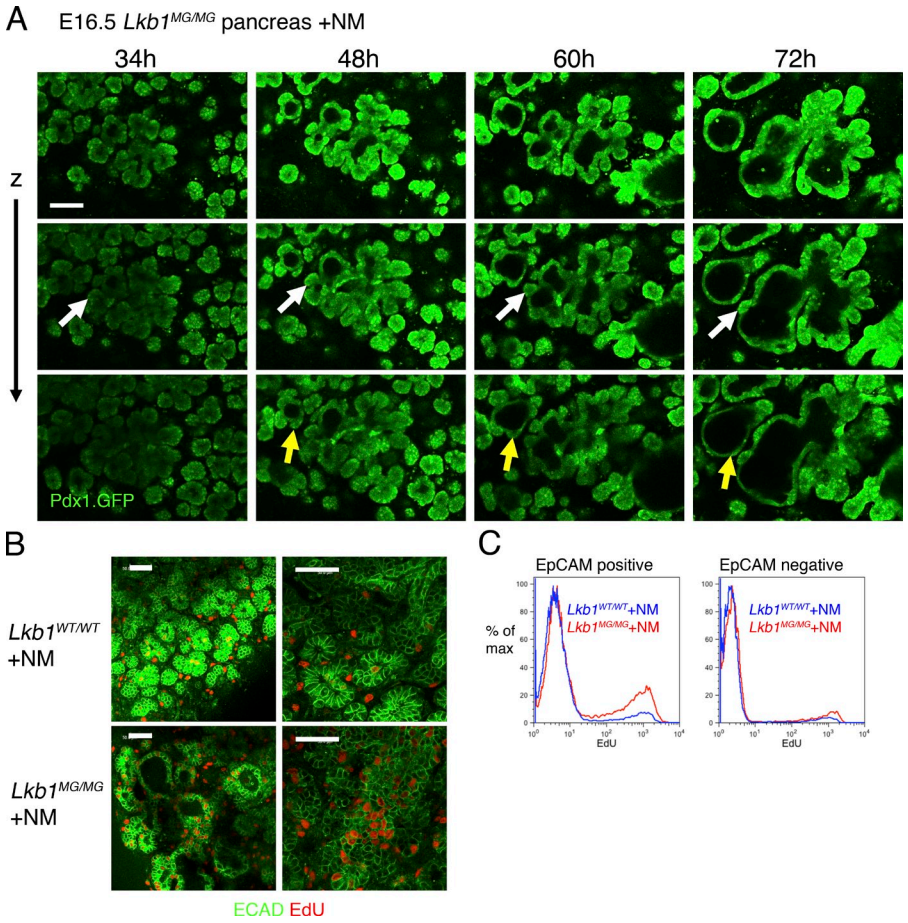

Figure 4. **Pancreatic cyst formation is dynamic and accompanied by increased cell proliferation.** (A) Time-lapse imaging of pancreatic cyst development. Serial images over 72 h of an E16.5 Lkb1$^{MG/MG}$ explant expressing Pdx1-GFP treated with 1 µM 1NMPP1. Cyst formation begins as a dilatation of the distal ductal compartment. Adjacent acinar structures can remain intact (white arrows) or can be seen coalescing with the wall of the cyst (yellow arrows). Bar, 100 µm. (B) Pancreatic cysts exhibit increased cell proliferation. Increased EdU (red) incorporation in E-cadherin (green)–positive cells forming a cyst in an Lkb1$^{MG/MG}$ explant (bottom) compared with an Lkb1$^{WT/WT}$ explant (top). Bars, 50 µm. (C) FACS analysis of pancreatic explants showing increase in EdU incorporation in the EpCAM-positive cells associated with Lkb1 inhibition. The data shown is from a single representative experiment out of five independent experiments.

In contrast, A-769662 treatment was unable to suppress cyst formation in pancreatic explants (Fig. 5 C). Moreover, the increased rate of EdU incorporation in epithelial cells lining cystic structures was unaltered by A-769662 (unpublished data). The failure of A-769662 to complement the defect was not a result of its inability to activate AMPK because the activator was effective at restoring or enhancing the phosphorylation of two AMPK substrates (ACC and Raptor; Fig. 5 D, lanes 7 and 8). Neither 1NMPP1 nor A-769662 had much effect on Lkb1$^{WT/WT}$ tissues. These results demonstrate that although A-769662 was capable of rescuing Lkb1-AMPK signaling in mutant explants, it was not able to rescue the morphogenesis defect in pancreas. Consistent with cyst formation being AMPK independent, direct inhibition of AMPK with compound C had no effect on embryonic pancreata (unpublished data). Thus, the Lkb1 kinase controls developmental morphogenesis in the lung and in the pancreas by distinct signaling pathways.

Pancreatic cysts induced by Lkb1 inhibition evolve into structures that resemble precancerous lesions

Given Lkb1's role as a tumor suppressor, we next asked if the pancreatic cysts might evolve into precancerous lesions such as pancreatic intraepithelial neoplasias (PanINs; Hruban et al., 2001). Lkb1$^{MG/MG}$ explants were treated continuously for extended periods with 1NMPP1. Cysts did not grow indefinitely and between 5 and 7 d they began to collapse inwardly, leading to accumulation of highly invaginated epithelial structures (Fig. 6 A) and an increase in the overall size of the explants with increased Ki67 staining and EdU incorporation (Fig. S3, A and B). Control explants (Lkb1$^{WT/WT}$ and Lkb1$^{WT/MG}$) exhibited slower growth and a more stereotypic pancreatic organization with acini and interconnecting tubules (Fig. 6 B). The collapsed epithelial structures exhibited features seen in PanIN lesions: tall columnar epithelial cells, extensive pseudostratification, papillary structures, luminal necrosis, nuclear crowding, and elongation, as well as overexpression of CD44v6 (Kure et al., 2012), an established marker of precancerous lesions that could be detected by both immunofluorescence and Western blot (Fig. 6 C). Strikingly, although these epithelial structures represented a significant departure from normal tissue architecture, cells comprising them retained intrinsic apical-basal polarity. EpCAM retained its basolateral distribution (Fig. 6 A) and Muc-1 remained apical, whereas ZO-1 staining illustrated a morphologically intact network of tight junctions (Fig. S3 C). Furthermore, despite the pseudostratification, the majority of the nuclei were basally positioned and mitotic figures (when observed) exhibited cell division parallel to the basement membrane. Thus, epithelial structures resulting from Lkb1 inhibition histologically resemble early stage PanINs that have not yet developed the widespread loss of polarity that characterizes late stage PanIN lesions (Hruban et al., 2006).

Because oncogenic K-Ras has been found in a large proportion of PanINs and is a major driver of progression to

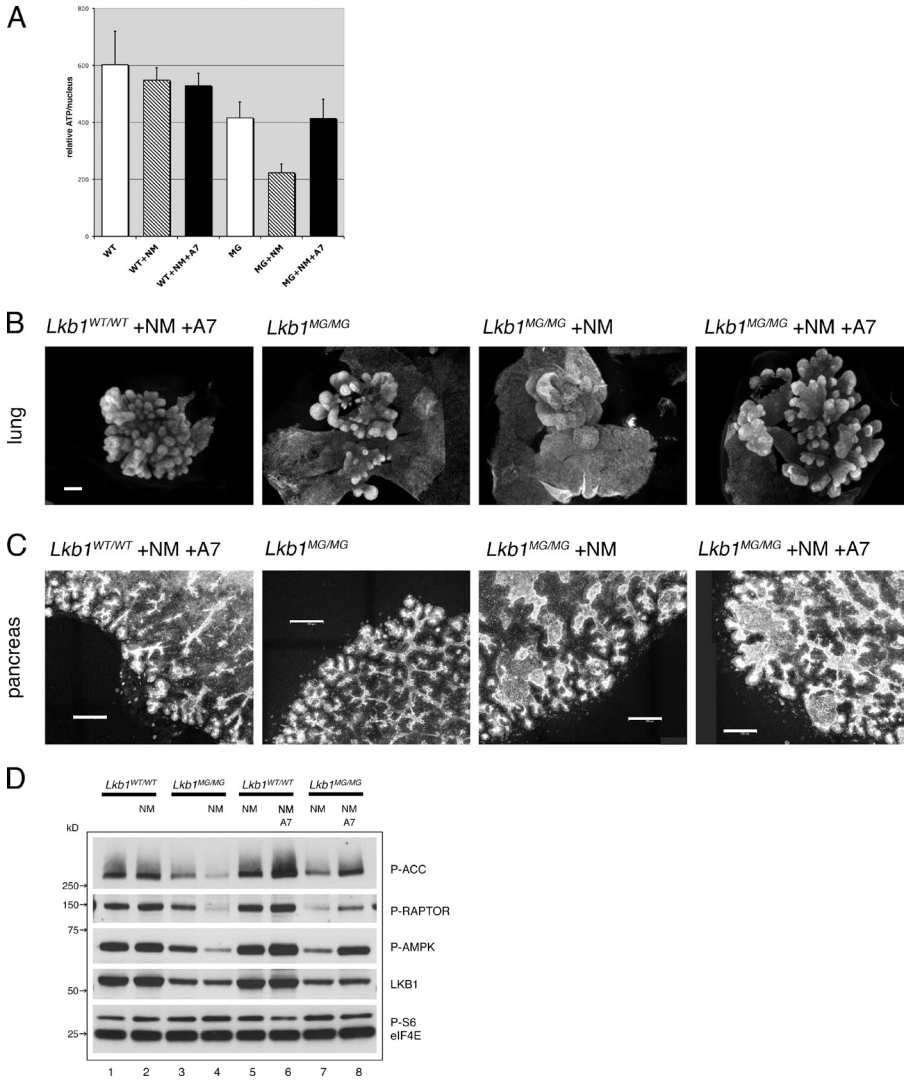

Figure 5. **Lung morphogenesis effects are AMPK dependent, whereas pancreatic cyst formation is AMPK independent.** (A) Lkb1$^{WT/WT}$ (WT) and Lkb1$^{MG/MG}$ (MG) MEFs were seeded into 96-well plates with DMSO or 1 µM 1NMPP1 or 1 µM 1NMPP1 and 100 µM A-769662. At 72 h, cell nuclei were counted using Vybrant green DNA stain and ATP levels were measured using CellTitre-Glo. Error bars represent standard deviations (n = 12). (B) Mesenchyme-free Lkb1$^{WT/WT}$ and Lkb1$^{MG/MG}$ lung epithelium were cultured with 1 µM 1NMPP1 and 100 µM A-769662. The branching defect induced by 1NMPP1 in the mesenchyme-free Lkb1$^{MG/MG}$ lung epithelium is reversed by the addition of A-769662. The images shown are E-cadherin–stained explants. Bar, 100 µm. (C) Pancreatic explants from E14.5 Lkb1$^{WT/WT}$ and Lkb1$^{MG/MG}$ were cultured with 1 µM 1NMPP1 and 100 µM A-769662. The cyst development induced by 1NMPP1 in the Lkb1$^{MG/MG}$ explant is not reversed by the addition of A-769662. The images shown are maximum projections across an 18-µm z-stack of ZO-1–stained explants. Bars, 100 µm. (D) Embryonic explants (pancreas) from Lkb1$^{WT/WT}$ (lanes 1, 2, 5, and 6) and Lkb1$^{MG/MG}$ (lanes 3, 4, 7, and 8) embryos were cultured ex vivo on transwell filters and incubated 2 h with DMSO (lanes 1 and 3) or 1 µM 1NMPP1 (lanes 2, 4, 5, and 7) or 1 µM 1NMPP1 and 100 µM A-769662 (lanes 6 and 8) before collecting lysates. Western blots were analyzed with antibodies to Phospho-ACC(Ser79), Phospho-RAPTOR(Ser792), Phospo-AMPKα(Thr172), Lkb1, Phospho-S6(Ser235/236), and eIF4E (as loading control).

pancreatic adenocarcinoma (Hingorani et al., 2003; Löhr et al., 2005), we introduced a mutant K-Ras allele to test whether this combination of oncogene and tumor suppressor loss would further impact cellular polarity and/or tissue organization. We produced Lkb1$^{MG/MG}$ embryos heterozygous for the lox.stop.lox KrasG12D allele. Pancreatic explants were infected with AAV. Cre.IRES.GFP to activate expression of KrasG12D. As shown in Fig. 7 A, a mosaic pattern of GFP expression was seen in an Lkb1$^{MG/MG}$Kras$^{LSL.G12D/WT}$ explant cultured with 1NMPP1 2 d after AAV infection. Comparison of GFP-positive and -negative cells with respect to morphology and polarity markers suggested that even acute activation of KrasG12D together with Lkb1 inhibition was still insufficient to drive a significant loss of intrinsic cell polarity. Experiments culturing explants 4 d after adeno-associated virus (AAV) infection showed similar cyst development as uninfected controls, again without overt loss of polarity. Similar results were found for explants expressing KrasG12D with wild-type Lkb1 (unpublished data).

Although the combined actions of oncogenic K-Ras and Lkb1 inhibition were insufficient to acutely disrupt polarity or induce an invasive phenotype, we asked if substituting Lkb1 with the loss of a different tumor suppressor would result in similar findings. We examined pancreatic explants in which the p16p19 locus (containing the tumor suppressors Ink4A and Arf) was deleted because mutations in this region are also commonly found in both PanINs and pancreatic adenocarcinoma (Hingorani et al., 2003; Abe et al., 2007). Although E14.5 pancreata from p16p19$^{-/-}$ and Kras$^{G12D/WT}$p16p19$^{-/-}$ were initially indistinguishable from each other (and wild-type pancreata), after culturing as explants for 5 d, the Kras$^{G12D/WT}$-p16p19$^{-/-}$ explants exhibited regions with irregular branching that appeared to coincide with increased proliferation as indicated by EdU incorporation (Fig. 7 B and Fig. S4 A). Over the next 2–4 d these regions demonstrated increasingly disrupted architecture that included luminal dilations that were, however, smaller and less dramatic than the cysts seen with Lkb1 inhibition. As with the epithelial structures induced by Lkb1 inhibition, tissue disorganization seen in Kras$^{G12D/WT}$-p16p19$^{-/-}$ explants was characterized by pseudostratification, nuclear crowding, and elongation (Figs. 7 C and S4 B). Therefore, as seen with Lkb1 inhibition, activation of mutant K-Ras together with loss of p16p19 led to changes in tissue architecture in pancreatic embryonic explants that phenotypically resembled precancerous lesions. Although the overall pattern

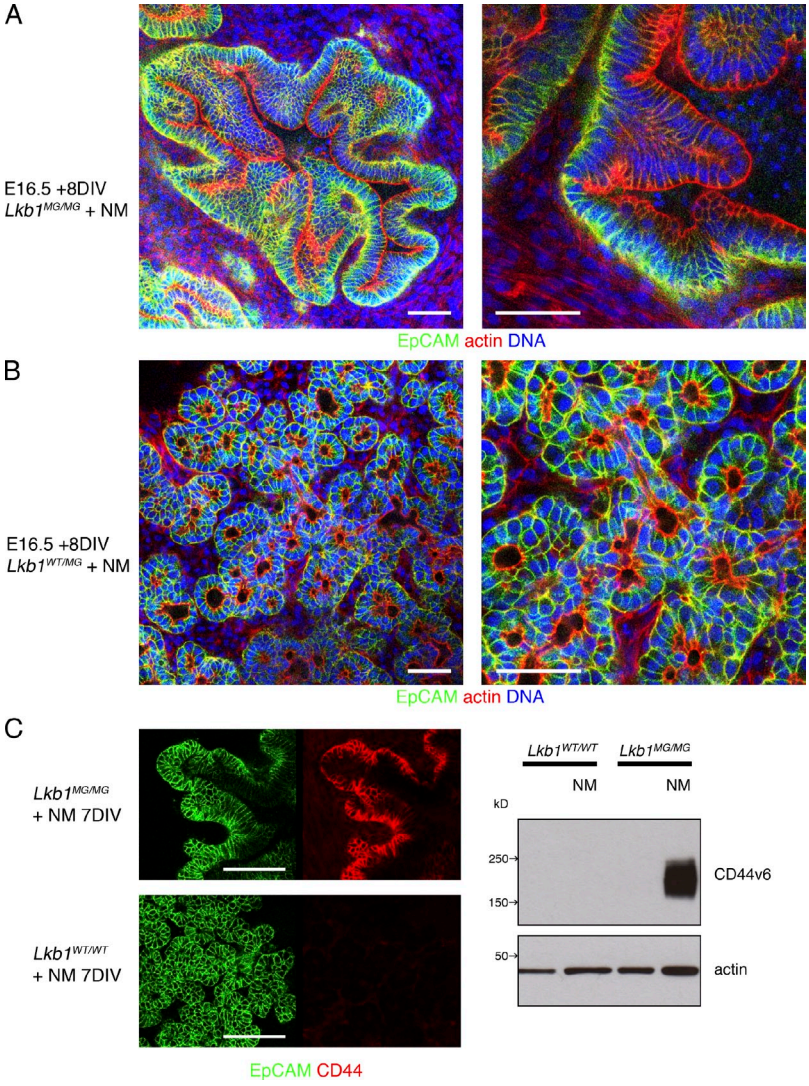

Figure 6. **Pancreatic cysts induced by Lkb1 inhibition evolve into structures that resemble precancerous PanIN lesions.** (A) E16.5 pancreatic explants were cultured on transwell filters for 8 DIV with 1 µM 1NMPP1. Lkb1$^{MG/MG}$ explants developed cysts that then evolved into highly invaginated epithelial structures composed of pseudostratified columnar cells. (B) Lkb1$^{WT/MG}$ explants were unaffected by the 1NMPP1 and retained their branched network of differentiating ductal and acinar cells. Tissues were fixed and processed for whole-mount confocal microscopy using Alexa Fluor 488 anti-EpCAM antibody, Alexa Fluor 546 phalloidin, and DAPI. (C) Lkb1$^{MG/MG}$ explants treated with 1NMPP1 dramatically overexpress CD44 as shown in whole-mount immunofluorescence (left) using anti-CD44 antibody (clone IM7) and in Western blots (right) of explant lysates probed with anti-CD44v6 antibody (clone 9A4). Bars: (A and B) 50 µm; (C) 100 µm.

of ZO-1 and Muc-1 staining was consistent with intact apical-basal polarity, E-cadherin mislocalization was observed in regions of the Kras$^{G12D/WT}$p16p19$^{-/-}$ explants where tissue organization was most severely disrupted (Fig. 7 C, arrows).

Discussion

By combining chemical genetics together with optimized methods for long-term culture of embryonic explants, we have begun to understand the mechanism of the tumor suppressor Lkb1 in the context of complex mammalian tissues. The accessibility of the explants makes it possible to conduct experiments with a temporal and spatial resolution normally possible only in cell lines while maintaining a physiologically relevant arrangement of multiple primary cell types within a native extracellular matrix. The approach with embryonic tissues complements and extends 3D culture systems (Leung and Brugge, 2012; Muthuswamy and Xue, 2012) and in vivo microscopy methodologies (Orth et al., 2011) and not only facilitates live cell imaging and genetic manipulation but also the use of specific small molecule inhibitors and agonists. Such agents could be used to compare the role of Lkb1 in different organ systems without complications caused by pharmacokinetic differences that limit in vivo studies. Although we concentrated on lung and pancreas, experiments with other tissues are possible and together would serve to conceptually extend the conditional Lkb1 knockout models that have been generated but only studied as end point assays in vivo.

Surprisingly, we found that Lkb1 kinase activity functions quite differently in the morphogenesis of different epithelial tissues. In the lung, we have defined a role for Lkb1 in branching morphogenesis that is epithelial cell autonomous. In contrast, Lkb1 inhibition in early stage pancreatic explants did not impact the branching and remodeling of the developing ductal plexus. Only at the later stages of pancreatic development did Lkb1 inhibition lead to a significant tissue defect characterized by epithelial cysts. Live imaging experiments revealed that cyst formation began with a rapid dilatation of the distal ductal compartment, suggesting that Lkb1 is involved in the stabilization of tissue architecture and possibly fluid flow, as opposed to regulating branching morphogenesis. Even more striking was the observation that only the lung branching defect appeared to be

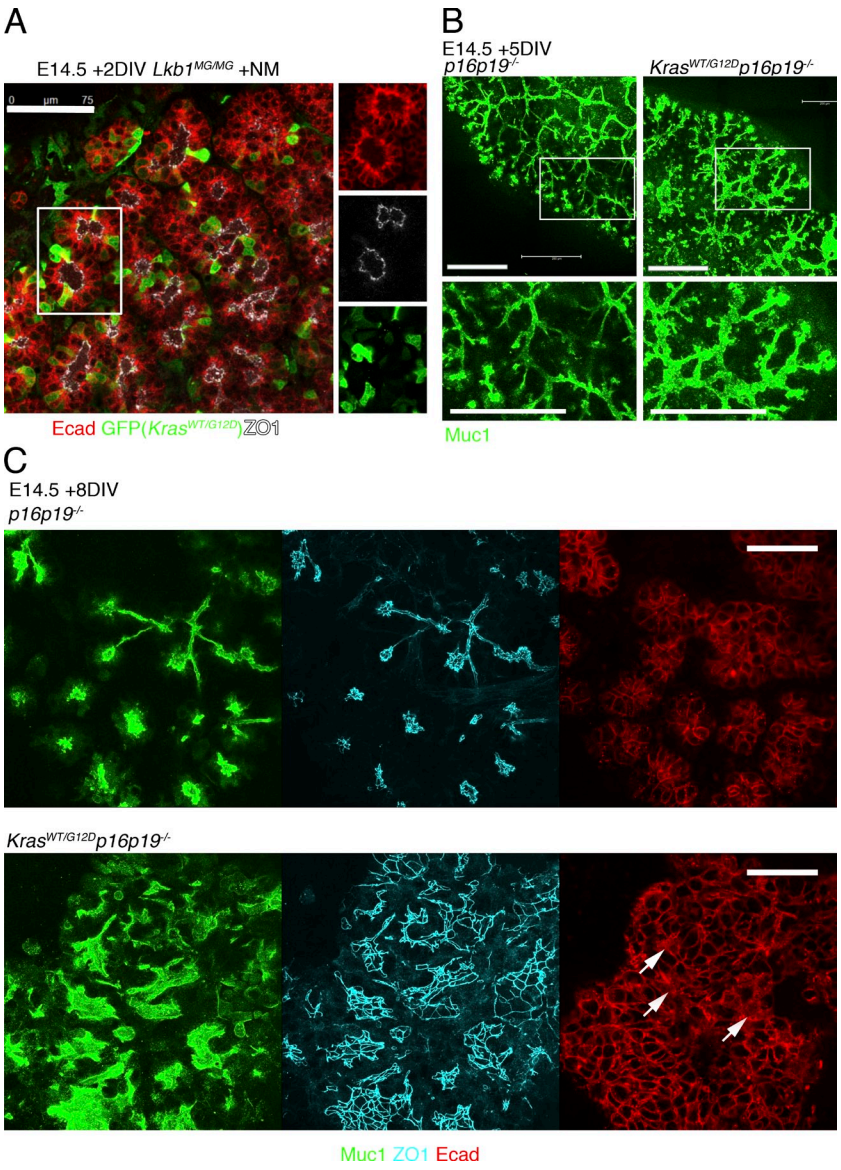

Figure 7. **Expression of mutant K-Ras with Lkb1 inhibition or p16p19 loss in embryonic pancreas cultured ex vivo.** (A) Pancreatic explants were harvested from E14.5 Lkb1$^{MG/MG}$ embryos that were heterozygous for lox.stop.lox KrasG12D, infected in vitro with AAV.Cre.IRES.GFP, and then cultured for two additional days with 1NMPP1. GFP-positive and -negative cells show similar morphology and pattern of E-cadherin and ZO-1 staining. GFP was detected with an anti-GFP antibody. (B) E14.5 p16p19$^{-/-}$ and Kras$^{G12D/WT}$p16p19$^{-/-}$(Pdx1-Cre) pancreatic explants were cultured for 5 d, fixed, and stained with Muc-1 antibody. Explants with Kras$^{G12D/WT}$ exhibit regions with irregular branching and luminal dilations. (C) E14.5 p16p19$^{-/-}$ and Kras$^{G12D/WT}$p16p19$^{-/-}$(Pdx1-Cre) pancreatic explants were cultured for 8 d, fixed, and stained with Muc-1, ZO-1, and E-cadherin antibodies. Explants with Kras$^{G12D/WT}$ exhibit regions of progressively disrupted tissue architecture and occasional cells with mislocalized E-cadherin (arrows). (Note: Muc-1 and ZO-1 are shown as maximum projections across a 10-µM z-stack; E-cadherin is a single section from the middle of the z-stack.) Bars: (A) 75 µM; (B) 200 µm; (C) 50 µm.

AMPK mediated, whereas the pancreas cyst formation is AMPK independent. This finding has now made it clear that targets beyond AMPK must be more seriously considered to understand the function of Lkb1 in morphogenesis and cancer. We are actively working to identify relevant Lkb1 targets using the ex vivo approach.

Given the previous connections between Lkb1 and cell polarity observed in various model organisms and cancer cell lines (Watts et al., 2000; Martin and St Johnston, 2003; Baas et al., 2004; Amin et al., 2009), we focused on determining whether disruption in intrinsic epithelial cell polarity preceded or accompanied the morphogenesis defects induced by Lkb1 inhibition. Contrary to expectations, for both lung and pancreas, our experiments consistently demonstrated that the steady-state distributions of various apical-basal polarity markers were unaffected by acute or longer-term inhibition of Lkb1 kinase activity. Similarly, Lkb1 deficiency in a zebrafish developmental model did not demonstrate polarity defects in either gut or eye (van der Velden et al., 2011), and conditional deletions of Lkb1 in mouse intestine (Shorning et al., 2009) and endometrium (Contreras et al., 2008) led to no obvious disruption in epithelial polarity. Other studies examining loss of Lkb1 in breast (McCarthy et al., 2009; Partanen et al., 2012), prostate (Pearson et al., 2008), and liver (Fu et al., 2011; Woods et al., 2011) have observed modest alterations in epithelial polarity, suggesting that tissue context modulates Lkb1 function.

Comparing the pancreatic cysts induced by Lkb1 inhibition and the cystic neoplasias that develop in the Pdx1-Cre–driven Lkb1 deletion mouse model (Hezel et al., 2008), although there is general agreement, we note some important differences between the two systems. Although Pdx1-Cre drives recombination in early pancreatic progenitors, the cysts in the conditional deletion model did not arise during embryogenesis but rather in the neonatal period. In contrast, we have shown that cyst induction by Lkb1 inhibition occurs in late but not early stage embryonic explants. In fact, by systematically harvesting explants at various developmental stages, we have found that cyst formation coincides with the secondary transition, a

wave of differentiation that begins around E14.5 (Villasenor et al., 2010). One possible explanation for this difference may relate to the acute and uniform nature of small molecule inhibition minimizing the chances for compensatory adaptations. Alternatively, the explant culture system may have introduced a factor that is permissive for cyst formation. In either event, the fundamental similarity of the two cystic phenotypes is impressive and strongly validates the chemical genetic approach to studying Lkb1.

Although the pancreatic explants examined here demonstrate intact apical-basal polarity in the face of Lkb1 inhibition, some junctional complex lateralization was reported for the conditional knockout (Hezel et al., 2008). This discrepancy may be the result of a small amount residual kinase activity from incomplete inhibition by 1NMPP1 or the possibility that Lkb1 may play a role in maintaining polarity independent of its kinase activity, perhaps as a scaffold for junctional components. In either case, the conclusion remains that pancreatic cysts induced from Lkb1 loss do not appear to reflect a defect in polarity. Moreover, as seen for *Drosophila melanogaster* (Lee et al., 2007; Mirouse et al., 2007), Lkb1 inactivation can render a tissue more susceptible to energy deprivation and this susceptibility may manifest as a partial alteration of cell organization as a secondary effect.

Although it is well established that Lkb1 is a tumor suppressor that participates in the pathogenesis of a wide range of cancers, the mechanism underlying this function remains poorly understood. We found that the pancreatic cysts induced by Lkb1 inhibition evolved into epithelial structures that resemble PanINs, the canonical precancerous lesions of the pancreas, based both on histological analysis and the expression of cancer-associated genes such as CD44. This suggests that for pancreas, Lkb1 has an important role suppressing early oncogenesis. We were thus led to ask whether Lkb1 inhibition can be combined with oncogene activation to further induce loss of polarity, invasiveness, or appearance of cancerous lesions in the embryonic explants. In several mouse tumor models, loss of Lkb1 clearly synergizes with mutant K-Ras to produce cancer (Ji et al., 2007; Morton et al., 2010). We therefore analyzed embryonic explants in which mutant endogenous K-Ras was activated together with Lkb1 inhibition but found no acute effects on polarity, cell shape, or migration, suggesting that additional genetic or epigenetic changes are required for transformation. For comparison, we examined the combination of mutant endogenous K-Ras with Ink4A/Arf (p16/p19) loss and found that despite a significant disruption of tissue architecture there was still no significant loss of polarity. Collectively, these results suggest that tissue architecture, even one that has undergone significant disorganization and metaplasia, is still able to resist, at least acutely, transformation by mutant K-Ras and loss of a single tumor suppressor. Only with additional "hits" are cells able to break free of the constraints imposed by the tissue and demonstrate the loss of polarity seen in carcinomas (Muthuswamy and Xue, 2012). The explant system now provides a unique approach to reconstructing the individual events that accompany the initiation of cancerous lesions.

To summarize, we have demonstrated that embryonic explants can be used to study the effects of tumor suppressors and oncogenes on the organization of complex mammalian tissues. Although carcinogenesis arises in adult tissues and not embryonic systems, the approach will be a valuable bridge between the observations made in cell lines with those made in animal models by providing a tissue platform that enables the visualization and detailed analysis of cell biological and genetic changes in tissues and single cells that are relevant to tumor initiation and transformation.

Materials and methods

Lkb1 vector construction

The construct for targeting the C57BL/6 Stk11 locus was made using recombineering (Warming et al., 2005), DNA synthesis, and standard molecular cloning techniques. After retrieving a genomic fragment containing Lkb1 from a C57BL/6 BAC (RP23 library) into pBlight-TK, the sequence 5′-GTGATGGAGTACTGCGTA-3′ within exon 3 was replaced with 5′-GTTGGGGGAATATTGCGTA-3′ to change Met129 to a glycine and replace a ScaI with an SspI site. A neomycin cassette flanked by loxp was then introduced into intron2. The final vector was confirmed by DNA sequencing and linearized. C57BL/6 C2 embryonic stem cells were targeted with standard methods and positive clones were transfected with Cre to remove the neomycin cassette. The modified embryonic stem cells were then injected into blastocysts and germline transmission was obtained by crossing the chimeras with C57BL/6 females.

Mouse strains

In addition to creating the $Lkb1^{MG}$ mouse, we used the following mouse strains: $Kras^{LSL-G12D}$ from T. Jacks (Massachusetts Institute of Technology, Cambridge, MA), $p16/p19^{fl/fl}$ from A. Berns (Netherlands Cancer Institute, Amsterdam, Netherlands), Pdx1-Cre from A. Lowy (University of Ohio, Athens, OH), and Pdx1-GFP from Edouard Stanley (Monash University, Clayton, Australia). Animals were housed and cared for according to guidelines from the Institutional Animal Care and Use Committee at Genentech.

Embryonic explant culture

Pancreas and individual lobes of the lungs were dissected from embryos harvested from time pregnancy setups. Embryonic explants were cultured on 0.4-µm polyester transwells (Corning) at the air–liquid interface in DMEM with 10% FCS, glutamine, and pen-strep. For longer-term cultures (>3 d), media was changed daily.

For mesenchyme-free cultures, lungs were dissected and incubated in Collagenase/Dispase (1 mg/ml for each) for 5–10 min at room temperature. Epithelial tissue was removed by mechanical dissection, transferred to transwells, and covered with 5–10 µl of 1:1 Matrigel/DME. After Matrigel was solidified, 400 µl of media (DMEM, 10% FCS, glutamine, pen-strep, and 200 ng/ml FGF7 or FGF1 [Invitrogen]) was added to top and bottom wells. In epithelium-mesenchyme transplant experiments, mesenchyme was positioned in contact with epithelial explants after addition of Matrigel and FGF was omitted from the culture media.

AAV infection

AAV8.2-Cre-IRES-GFP and control AAV8.2 GFP virus (Virovek) in a 10–20-µl volume of serum-free media was added directly to explants in the transwell plates. The explants were fixed at various time points after infection and then stained with anti-GFP antibody together with other primary antibodies.

Whole-mount immunofluorescence

Embryonic explants were fixed in 4% paraformaldehyde, permeabilized in PBS with 2% BSA, 0.1% saponin, or 0.1% Triton X-100. After staining with primary antibodies and fluorescently labeled secondary antibodies, explants were mounted and imaged with a laser confocal microscope (SP5; Leica) with integrated photomultiplier detectors. Objective lenses were a 40×, 1.25 NA, HCX PL APO oil immersion objective or a 63×, 1.40 NA, HCX PL APO oil immersion objective. Images shown are representative of multiple independent experiments ($n \geq 5$) with littermate explants that were cultured, stained, and imaged under identical conditions and settings.

Live imaging

Explants cultured on the transwell filters could be directly imaged using conventional phase and fluorescence microscopy. For time-lapse confocal imaging on the SP5, filters with attached pancreatic explants were removed from the plastic support, inverted, and placed in a WillCo glass bottom dish containing media. In between image acquisitions the pancreatic explants were returned to a transwell for culturing at the air–liquid interface. For continuous live imaging (Video 1) of multiple explants in parallel within a transwell plate, we used an Eclipse Ti-E with Perfect Focus hardware autofocus (Nikon), 10× Plan Flour 0.3 NA phase-contrast objective, Revolution DSD white light spinning disk confocal (Andor Technology), Prior LumenPRO 200W metal halide illumination system (Prior Scientific), Clara charge-coupled device camera (1,392 × 1,024, 6.45 µm pixels; Andor Technology), and IQ2 software (Andor Technology). Temperature, humidity, and CO_2 control was provided by an environmental chamber (Okolab). Video 1 is representative of multiple independent experiments ($n \geq 3$).

Reagents

Antibodies used were anti-E-cadherin (DECMA-1 [Santa Cruz Biotechnology, Inc.]; clone 36/E-cadherin [BD]); anti-ZO-1 (R40.76; Santa Cruz Biotechnology, Inc.); anti–Muc-1 (rabbit polyclonal; Abcam); anti-EpCAM (G8.8; BioLegend); anti-Phospho-ACC(Ser79) (rabbit polyclonal; Cell Signaling Technology), anti-ACC (C83B10; Cell Signaling Technology), anti-Phospho-AMPKα(Thr172) (40H9; Cell Signaling Technology), anti-AMPKα (23A3; Cell Signaling Technology), anti-Lkb1 (D60C5; Cell Signaling Technology), anti-Phospho-Raptor(Ser792) (rabbit polyclonal; Cell Signaling Technology), anti-Phospho-S6(Ser235/236) (D57.2.2E; Cell Signaling Technology), anti-eIF4E (rabbit polyclonal; Cell Signaling Technology), anti-CD44 (IM7; BioLegend), anti-CD44v6 (9A4; AbD Serotec), anti-Ki67 (B56; BD), anti–active caspase-3 (rabbit polyclonal; Promega), anti-gp135 (G. Ojakian, State University of New York, Brooklyn, NY), anti-gp58 (hybridoma from American Type Culture Collection), anti-GFP (Invitrogen), anti–actin-HRP (Santa Cruz Biotechnology, Inc.), various Alexa Fluor–conjugated secondary antibodies (Invitrogen), and various HRP-conjugated secondary antibodies (GE Healthcare). Other reagents used were: Alexa Fluor phalloidin (Invitrogen), DAPI (Cell Signaling Technology), Click-iT EdU Alexa Fluor kit (Invitrogen), SYTOX Orange Nucleic Acid Stain (Life technologies), AICAR (Cell Signaling Technology), A-769662 (Tocris Bioscience), 1NMPP1 (EMD Millipore), 1NaPP1 (provided by the Shokat laboratory, University of California, San Francisco, San Francisco, CA).

Cell culture

MDCK II cells were maintained in Dulbecco's MEM with low glucose supplemented with 10% FCS, 2 mM L-glutamine, penicillin, and streptomycin at 37°C, and 5% CO_2. For the monolayer experiments, cells were seeded at a density of 5×10^5 for each 12-mm 0.4-µm polyester filter. For the spheroid experiments, 45 µl of a 1:1 mixture of 10^4 cells in media to Matrigel (9–10 mg/ml; BD) was added to each well of a 96-well plate, incubated 30–45 min at 37°C, and then 100 µl of media was added to each well.

Primary MEFs were prepared from E12.5–13.5 embryos and were maintained in Dulbecco's MEM with high glucose supplemented with 10% FCS, 2 mM L-glutamine, penicillin, and streptomycin at 37°C, and 5% CO_2.

Lkb1 knockdown with shRNA

Oligonucleotides targeting the sequence 5′-GGGACAACATCTACAAGTTGT-3′ in Lkb1 mRNA were synthesized, annealed, and ligated to the LTRH1-puro retroviral vector. Retrovirus was produced in GP2-293 cells and MDCK cells were infected and selected in puromycin as previously described (Francis et al., 2011).

Flow cytometry

After digesting explants in Trypsin EDTA for 30–40 min, cells were stained with anti-EpCAM antibody on ice, PFA fixed, and processed for EdU labeling (Click-iT EdU Alexa Fluor kit), and then analyzed on a Canto-II (BD). Experiment shown is representative of multiple independent experiments ($n = 5$).

Western blot

Protein concentrations of tissue and cell lysates were determined by BCA assay (Thermo Fisher Scientific). Samples in LDS sample buffer plus β-mercaptoethanol were heated to 95°C for 5 min before separation by electrophoresis using NuPAGE 4–12% Bis Tris gels (Invitrogen). Proteins were transferred to nitrocellulose membranes overnight, membranes were blocked in TBS buffer with 0.1% Tween and 5% Blotto before incubating overnight at 4°C with primary antibodies in TBS buffer with 0.1% Tween and 2% BSA. Primary antibodies were detected with HRP-conjugated secondary antibodies and ECL reagents (Thermo Fisher Scientific). Experiments shown are representative of multiple independent experiments ($n \geq 3$).

Online supplemental material

Fig. S1 shows biochemical and RT-PCR characterization of the Lkb1 ASKA allele in cell lines. Fig. S2 shows that Lkb1 inhibition did not result in increased cell death in pancreatic explants. Fig. S3 shows that Lkb1 inhibition results in increased proliferation in the PanIN-like lesions without loss of apical-basal polarity. Fig. S4 shows that mutant K-Ras together with loss of p16/p19 increases cell proliferation and induces disruptions in tissue architecture in pancreatic explants. Fig. S5 shows quantification of morphogenesis defect in lung explants and proliferation in pancreas explants induced by Lkb1 inhibition. Video 1 shows fluorescence time-lapse imaging of pancreatic cyst formation. Table S1 summarizes the FACS experiments examining EdU-positive cells in pancreatic explants. Table S2 summarizes the mesenchyme-free lung epithelial culture experiments. Table S3 shows quantification of cyst number and size in pancreatic explants. Online supplemental material is available at http://www.jcb.org/cgi/content/full/jcb.201208080/DC1.

We would like to thank members of the Mellman laboratory for their support and useful discussions, Fred de Sauvage for helpful comments on the manuscript, Soren Warming for advice on construct generation, Meron Roose-Girma and Embryonic Stem Cell facility for generating the knockin mouse, and all the dedicated staff in the Genentech genotyping and animal facility for their expert support.

All authors are employees of Genentech, a member of the Roche group.

Submitted: 14 August 2012
Accepted: 26 November 2012

References

Abe, K., K. Suda, A. Arakawa, S. Yamasaki, H. Sonoue, K. Mitani, and B. Nobukawa. 2007. Different patterns of p16INK4A and p53 protein expressions in intraductal papillary-mucinous neoplasms and pancreatic intraepithelial neoplasia. *Pancreas*. 34:85–91. http://dx.doi.org/10.1097/01.mpa.0000240608.56806.0a

Alessi, D.R., K. Sakamoto, and J.R. Bayascas. 2006. LKB1-dependent signaling pathways. *Annu. Rev. Biochem.* 75:137–163. http://dx.doi.org/10.1146/annurev.biochem.75.103004.142702

Amin, N., A. Khan, D. St Johnston, I. Tomlinson, S. Martin, J. Brenman, and H. McNeill. 2009. LKB1 regulates polarity remodeling and adherens junction formation in the *Drosophila* eye. *Proc. Natl. Acad. Sci. USA*. 106:8941–8946. http://dx.doi.org/10.1073/pnas.0812469106

Baas, A.F., J. Kuipers, N.N. van der Wel, E. Batlle, H.K. Koerten, P.J. Peters, and H.C. Clevers. 2004. Complete polarization of single intestinal epithelial cells upon activation of LKB1 by STRAD. *Cell*. 116:457–466. http://dx.doi.org/10.1016/S0092-8674(04)00114-X

Bardeesy, N., M. Sinha, A.F. Hezel, S. Signoretti, N.A. Hathaway, N.E. Sharpless, M. Loda, D.R. Carrasco, and R.A. DePinho. 2002. Loss of the Lkb1 tumour suppressor provokes intestinal polyposis but resistance to transformation. *Nature*. 419:162–167. http://dx.doi.org/10.1038/nature01045

Barnes, A.P., B.N. Lilley, Y.A. Pan, L.J. Plummer, A.W. Powell, A.N. Raines, J.R. Sanes, and F. Polleux. 2007. LKB1 and SAD kinases define a pathway required for the polarization of cortical neurons. *Cell*. 129:549–563. http://dx.doi.org/10.1016/j.cell.2007.03.025

Bishop, A.C., J.A. Ubersax, D.T. Petsch, D.P. Matheos, N.S. Gray, J. Blethrow, E. Shimizu, J.Z. Tsien, P.G. Schultz, M.D. Rose, et al. 2000. A chemical switch for inhibitor-sensitive alleles of any protein kinase. *Nature*. 407:395–401. http://dx.doi.org/10.1038/35030148

Cardoso, W.V., A. Itoh, H. Nogawa, I. Mason, and J.S. Brody. 1997. FGF-1 and FGF-7 induce distinct patterns of growth and differentiation in embryonic lung epithelium. *Dev. Dyn.* 208:398–405. http://dx.doi.org/10.1002/(SICI)1097-0177(199703)208:3<398::AID-AJA10>3.0.CO;2-X

Cheng, H., P. Liu, Z.C. Wang, L. Zou, S. Santiago, V. Garbitt, O.V. Gjoerup, J.D. Iglehart, A. Miron, A.L. Richardson, et al. 2009. SIK1 couples LKB1 to p53-dependent anoikis and suppresses metastasis. *Sci. Signal.* 2:ra35. http://dx.doi.org/10.1126/scisignal.2000369

Contreras, C.M., S. Gurumurthy, J.M. Haynie, L.J. Shirley, E.A. Akbay, S.N. Wingo, J.O. Schorge, R.R. Broaddus, K.K. Wong, N. Bardeesy, and D.H. Castrillon. 2008. Loss of Lkb1 provokes highly invasive endometrial adenocarcinomas. *Cancer Res.* 68:759–766. http://dx.doi.org/10.1158/0008-5472.CAN-07-5014

Francis, S.S., J. Sfakianos, B. Lo, and I. Mellman. 2011. A hierarchy of signals regulates entry of membrane proteins into the ciliary membrane domain in epithelial cells. *J. Cell Biol.* 193:219–233. http://dx.doi.org/10.1083/jcb.201009001

Fu, D., Y. Wakabayashi, J. Lippincott-Schwartz, and I.M. Arias. 2011. Bile acid stimulates hepatocyte polarization through a cAMP-Epac-MEK-LKB1-AMPK pathway. *Proc. Natl. Acad. Sci. USA*. 108:1403–1408. http://dx.doi.org/10.1073/pnas.1018376108

Göransson, O., A. McBride, S.A. Hawley, F.A. Ross, N. Shpiro, M. Foretz, B. Viollet, D.G. Hardie, and K. Sakamoto. 2007. Mechanism of action of A-769662, a valuable tool for activation of AMP-activated protein kinase. *J. Biol. Chem.* 282:32549–32560. http://dx.doi.org/10.1074/jbc.M706536200

Hawley, S.A., J. Boudeau, J.L. Reid, K.J. Mustard, L. Udd, T.P. Mäkelä, D.R. Alessi, and D.G. Hardie. 2003. Complexes between the LKB1 tumor suppressor, STRAD alpha/beta and MO25 alpha/beta are upstream kinases in the AMP-activated protein kinase cascade. *J. Biol.* 2:28. http://dx.doi.org/10.1186/1475-4924-2-28

Hearle, N., V. Schumacher, F.H. Menko, S. Olschwang, L.A. Boardman, J.J. Gille, J.J. Keller, A.M. Westerman, R.J. Scott, W. Lim, et al. 2006. Frequency and spectrum of cancers in the Peutz-Jeghers syndrome. *Clin. Cancer Res.* 12:3209–3215. http://dx.doi.org/10.1158/1078-0432.CCR-06-0083

Hemminki, A., D. Markie, I. Tomlinson, E. Avizienyte, S. Roth, A. Loukola, G. Bignell, W. Warren, M. Aminoff, P. Höglund, et al. 1998. A serine/threonine kinase gene defective in Peutz-Jeghers syndrome. *Nature*. 391:184–187. http://dx.doi.org/10.1038/34432

Hezel, A.F., S. Gurumurthy, Z. Granot, A. Swisa, G.C. Chu, G. Bailey, Y. Dor, N. Bardeesy, and R.A. Depinho. 2008. Pancreatic LKB1 deletion leads to acinar polarity defects and cystic neoplasms. *Mol. Cell. Biol.* 28:2414–2425. http://dx.doi.org/10.1128/MCB.01621-07

Hingorani, S.R., E.F. Petricoin, A. Maitra, V. Rajapakse, C. King, M.A. Jacobetz, S. Ross, T.P. Conrads, T.D. Veenstra, B.A. Hitt, et al. 2003. Preinvasive and invasive ductal pancreatic cancer and its early detection in the mouse. *Cancer Cell*. 4:437–450. http://dx.doi.org/10.1016/S1535-6108(03)00309-X

Holland, A.M., S.J. Micallef, X. Li, A.G. Elefanty, and E.G. Stanley. 2006. A mouse carrying the green fluorescent protein gene targeted to the Pdx1 locus facilitates the study of pancreas development and function. *Genesis*. 44:304–307. http://dx.doi.org/10.1002/dvg.20214

Hruban, R.H., N.V. Adsay, J. Albores-Saavedra, C. Compton, E.S. Garrett, S.N. Goodman, S.E. Kern, D.S. Klimstra, G. Klöppel, D.S. Longnecker, et al. 2001. Pancreatic intraepithelial neoplasia: a new nomenclature and classification system for pancreatic duct lesions. *Am. J. Surg. Pathol.* 25:579–586. http://dx.doi.org/10.1097/00000478-200105000-00003

Hruban, R.H., N.V. Adsay, J. Albores-Saavedra, M.R. Anver, A.V. Biankin, G.P. Boivin, E.E. Furth, T. Furukawa, A. Klein, D.S. Klimstra, et al. 2006. Pathology of genetically engineered mouse models of pancreatic exocrine cancer: consensus report and recommendations. *Cancer Res.* 66:95–106. http://dx.doi.org/10.1158/0008-5472.CAN-05-2168

Huang, X., S. Wullschleger, N. Shpiro, V.A. McGuire, K. Sakamoto, Y.L. Woods, W. McBurnie, S. Fleming, and D.R. Alessi. 2008. Important role of the LKB1-AMPK pathway in suppressing tumorigenesis in PTEN-deficient mice. *Biochem. J.* 412:211–221. http://dx.doi.org/10.1042/BJ20080557

Jeghers, H., V.A. McKusick, and K.H. Katz. 1949. Generalized intestinal polyposis and melanin spots of the oral mucosa, lips and digits; a syndrome of diagnostic significance. *N. Engl. J. Med.* 241:1031–1036. http://dx.doi.org/10.1056/NEJM194912292412601

Jenne, D.E., H. Reimann, J. Nezu, W. Friedel, S. Loff, R. Jeschke, O. Müller, W. Back, and M. Zimmer. 1998. Peutz-Jeghers syndrome is caused by mutations in a novel serine threonine kinase. *Nat. Genet.* 18:38–43. http://dx.doi.org/10.1038/ng0198-38

Ji, H., M.R. Ramsey, D.N. Hayes, C. Fan, K. McNamara, P. Kozlowski, C. Torrice, M.C. Wu, T. Shimamura, S.A. Perera, et al. 2007. LKB1 modulates lung cancer differentiation and metastasis. *Nature*. 448:807–810. http://dx.doi.org/10.1038/nature06030

Jishage, K., J. Nezu, Y. Kawase, T. Iwata, M. Watanabe, A. Miyoshi, A. Ose, K. Habu, T. Kake, N. Kamada, et al. 2002. Role of Lkb1, the causative gene of Peutz-Jegher's syndrome, in embryogenesis and polyposis. *Proc. Natl. Acad. Sci. USA*. 99:8903–8908.

Katajisto, P., K. Vaahtomeri, N. Ekman, E. Ventelä, A. Ristimäki, N. Bardeesy, R. Feil, R.A. DePinho, and T.P. Mäkelä. 2008. LKB1 signaling in mesenchymal cells required for suppression of gastrointestinal polyposis. *Nat. Genet.* 40:455–459. http://dx.doi.org/10.1038/ng.98

Kemphues, K.J., J.R. Priess, D.G. Morton, and N.S. Cheng. 1988. Identification of genes required for cytoplasmic localization in early *C. elegans* embryos. *Cell*. 52:311–320. http://dx.doi.org/10.1016/S0092-8674(88)80024-2

Kure, S., Y. Matsuda, M. Hagio, J. Ueda, Z. Naito, and T. Ishiwata. 2012. Expression of cancer stem cell markers in pancreatic intraepithelial neoplasias and pancreatic ductal adenocarcinomas. *Int. J. Oncol.* 41:1314–1324.

Lee, J.H., H. Koh, M. Kim, Y. Kim, S.Y. Lee, R.E. Karess, S.H. Lee, M. Shong, J.M. Kim, J. Kim, and J. Chung. 2007. Energy-dependent regulation of cell structure by AMP-activated protein kinase. *Nature*. 447:1017–1020. http://dx.doi.org/10.1038/nature05828

Leung, C.T., and J.S. Brugge. 2012. Outgrowth of single oncogene-expressing cells from suppressive epithelial environments. *Nature*. 482:410–413. http://dx.doi.org/10.1038/nature10826

Lizcano, J.M., O. Göransson, R. Toth, M. Deak, N.A. Morrice, J. Boudeau, S.A. Hawley, L. Udd, T.P. Mäkelä, D.G. Hardie, and D.R. Alessi. 2004. LKB1 is a master kinase that activates 13 kinases of the AMPK subfamily, including MARK/PAR-1. *EMBO J.* 23:833–843. http://dx.doi.org/10.1038/sj.emboj.7600110

Löhr, M., G. Klöppel, P. Maisonneuve, A.B. Lowenfels, and J. Lüttges. 2005. Frequency of K-ras mutations in pancreatic intraductal neoplasias associated with pancreatic ductal adenocarcinoma and chronic pancreatitis: a meta-analysis. *Neoplasia*. 7:17–23. http://dx.doi.org/10.1593/neo.04445

Martin, S.G., and D. St Johnston. 2003. A role for *Drosophila* LKB1 in anterior-posterior axis formation and epithelial polarity. *Nature*. 421:379–384. http://dx.doi.org/10.1038/nature01296

McCarthy, A., C.J. Lord, K. Savage, A. Grigoriadis, D.P. Smith, B. Weigelt, J.S. Reis-Filho, and A. Ashworth. 2009. Conditional deletion of the Lkb1 gene in the mouse mammary gland induces tumour formation. *J. Pathol.* 219:306–316. http://dx.doi.org/10.1002/path.2599

Mehenni, H., N. Resta, J.G. Park, M. Miyaki, G. Guanti, and M.C. Costanza. 2006. Cancer risks in LKB1 germline mutation carriers. *Gut*. 55:984–990. http://dx.doi.org/10.1136/gut.2005.082990

Metzger, R.J., O.D. Klein, G.R. Martin, and M.A. Krasnow. 2008. The branching programme of mouse lung development. *Nature*. 453:745–750. http://dx.doi.org/10.1038/nature07005

Mirouse, V., L.L. Swick, N. Kazgan, D. St Johnston, and J.E. Brenman. 2007. LKB1 and AMPK maintain epithelial cell polarity under energetic stress. *J. Cell Biol.* 177:387–392. http://dx.doi.org/10.1083/jcb.200702053

Miyoshi, H., M. Nakau, T.O. Ishikawa, M.F. Seldin, M. Oshima, and M.M. Taketo. 2002. Gastrointestinal hamartomatous polyposis in Lkb1 heterozygous knockout mice. *Cancer Res.* 62:2261–2266.

Morton, J.P., N.B. Jamieson, S.A. Karim, D. Athineos, R.A. Ridgway, C. Nixon, C.J. McKay, R. Carter, V.G. Brunton, M.C. Frame, et al. 2010. LKB1 haploinsufficiency cooperates with Kras to promote pancreatic cancer through suppression of p21-dependent growth arrest. *Gastroenterology*. 139:586–597: 597: e1–e6. http://dx.doi.org/10.1053/j.gastro.2010.04.055

Muthuswamy, S.K., and B. Xue. 2012. Cell polarity as a regulator of cancer cell behavior plasticity. *Annu. Rev. Cell Dev. Biol.* 28:599–625. http://dx.doi.org/10.1146/annurev-cellbio-092910-154244

Nogawa, H., and T. Ito. 1995. Branching morphogenesis of embryonic mouse lung epithelium in mesenchyme-free culture. *Development*. 121:1015–1022.

Orth, J.D., R.H. Kohler, F. Foijer, P.K. Sorger, R. Weissleder, and T.J. Mitchison. 2011. Analysis of mitosis and antimitotic drug responses in tumors by in vivo microscopy and single-cell pharmacodynamics. *Cancer Res.* 71:4608–4616. http://dx.doi.org/10.1158/0008-5472.CAN-11-0412

Partanen, J.I., T.A. Tervonen, M. Myllynen, E. Lind, M. Imai, P. Katajisto, G.J. Dijkgraaf, P.E. Kovanen, T.P. Mäkelä, Z. Werb, and J. Klefström. 2012. Tumor suppressor function of Liver kinase B1 (Lkb1) is linked to regulation of epithelial integrity. *Proc. Natl. Acad. Sci. USA*. 109:E388–E397. http://dx.doi.org/10.1073/pnas.1120421109

Pearson, H.B., A. McCarthy, C.M. Collins, A. Ashworth, and A.R. Clarke. 2008. Lkb1 deficiency causes prostate neoplasia in the mouse. *Cancer Res.* 68:2223–2232. http://dx.doi.org/10.1158/0008-5472.CAN-07-5169

Puri, S., and M. Hebrok. 2007. Dynamics of embryonic pancreas development using real-time imaging. *Dev. Biol.* 306:82–93. http://dx.doi.org/10.1016/j.ydbio.2007.03.003

Rossi, D.J., A. Ylikorkala, N. Korsisaari, R. Salovaara, K. Luukko, V. Launonen, M. Henkemeyer, A. Ristimaki, L.A. Aaltonen, and T.P. Makela. 2002. Induction of cyclooxygenase-2 in a mouse model of Peutz-Jeghers polyposis. *Proc. Natl. Acad. Sci. USA*. 99:12327–12332. http://dx.doi.org/10.1073/pnas.192301399

Saadat, I., H. Higashi, C. Obuse, M. Umeda, N. Murata-Kamiya, Y. Saito, H. Lu, N. Ohnishi, T. Azuma, A. Suzuki, et al. 2007. *Helicobacter pylori* CagA targets PAR1/MARK kinase to disrupt epithelial cell polarity. *Nature*. 447:330–333. http://dx.doi.org/10.1038/nature05765

Sahin, F., A. Maitra, P. Argani, N. Sato, N. Maehara, E. Montgomery, M. Goggins, R.H. Hruban, and G.H. Su. 2003. Loss of Stk11/Lkb1 expression in pancreatic and biliary neoplasms. *Mod. Pathol.* 16:686–691. http://dx.doi.org/10.1097/01.MP.0000075645.97329.86

Sanchez-Cespedes, M. 2007. A role for LKB1 gene in human cancer beyond the Peutz-Jeghers syndrome. *Oncogene*. 26:7825–7832. http://dx.doi.org/10.1038/sj.onc.1210594

Sanders, M.J., Z.S. Ali, B.D. Hegarty, R. Heath, M.A. Snowden, and D. Carling. 2007. Defining the mechanism of activation of AMP-activated protein kinase by the small molecule A-769662, a member of the thienopyridone family. *J. Biol. Chem.* 282:32539–32548. http://dx.doi.org/10.1074/jbc.M706543200

Shaw, R.J., M. Kosmatka, N. Bardeesy, R.L. Hurley, L.A. Witters, R.A. DePinho, and L.C. Cantley. 2004. The tumor suppressor LKB1 kinase directly activates AMP-activated kinase and regulates apoptosis in response to energy stress. *Proc. Natl. Acad. Sci. USA*. 101:3329–3335. http://dx.doi.org/10.1073/pnas.0308061100

Shorning, B.Y., J. Zabkiewicz, A. McCarthy, H.B. Pearson, D.J. Winton, O.J. Sansom, A. Ashworth, and A.R. Clarke. 2009. Lkb1 deficiency alters goblet and paneth cell differentiation in the small intestine. *PLoS ONE*. 4:e4264. http://dx.doi.org/10.1371/journal.pone.0004264

ten Klooster, J.P., M. Jansen, J. Yuan, V. Oorschot, H. Begthel, V. Di Giacomo, F. Colland, J. de Koning, M.M. Maurice, P. Hornbeck, and H. Clevers. 2009. Mst4 and Ezrin induce brush borders downstream of the Lkb1/Strad/Mo25 polarization complex. *Dev. Cell*. 16:551–562. http://dx.doi.org/10.1016/j.devcel.2009.01.016

van der Velden, Y.U., L. Wang, J. Zevenhoven, E. van Rooijen, M. van Lohuizen, R.H. Giles, H. Clevers, and A.P. Haramis. 2011. The serine-threonine kinase LKB1 is essential for survival under energetic stress in zebrafish. *Proc. Natl. Acad. Sci. USA*. 108:4358–4363. http://dx.doi.org/10.1073/pnas.1010210108

Villasenor, A., D.C. Chong, M. Henkemeyer, and O. Cleaver. 2010. Epithelial dynamics of pancreatic branching morphogenesis. *Development*. 137:4295–4305. http://dx.doi.org/10.1242/dev.052993

Warming, S., N. Costantino, D.L. Court, N.A. Jenkins, and N.G. Copeland. 2005. Simple and highly efficient BAC recombineering using galK selection. *Nucleic Acids Res.* 33:e36. http://dx.doi.org/10.1093/nar/gni035

Watts, J.L., D.G. Morton, J. Bestman, and K.J. Kemphues. 2000. The *C. elegans* par-4 gene encodes a putative serine-threonine kinase required for establishing embryonic asymmetry. *Development*. 127:1467–1475.

Woods, A., A.J. Heslegrave, P.J. Muckett, A.P. Levene, M. Clements, M. Mobberley, T.A. Ryder, S. Abu-Hayyeh, C. Williamson, R.D. Goldin, et al. 2011. LKB1 is required for hepatic bile acid transport and canalicular membrane integrity in mice. *Biochem. J.* 434:49–60. http://dx.doi.org/10.1042/BJ20101721

Ylikorkala, A., D.J. Rossi, N. Korsisaari, K. Luukko, K. Alitalo, M. Henkemeyer, and T.P. Mäkelä. 2001. Vascular abnormalities and deregulation of VEGF in Lkb1-deficient mice. *Science*. 293:1323–1326. http://dx.doi.org/10.1126/science.1062074

Zagórska, A., M. Deak, D.G. Campbell, S. Banerjee, M. Hirano, S. Aizawa, A.R. Prescott, and D.R. Alessi. 2010. New roles for the LKB1-NUAK pathway in controlling myosin phosphatase complexes and cell adhesion. *Sci. Signal.* 3:ra25. http://dx.doi.org/10.1126/scisignal.2000616

Zeng, P.Y., and S.L. Berger. 2006. LKB1 is recruited to the p21/WAF1 promoter by p53 to mediate transcriptional activation. *Cancer Res.* 66:10701–10708. http://dx.doi.org/10.1158/0008-5472.CAN-06-0999

Zhang, C., D.M. Kenski, J.L. Paulson, A. Bonshtien, G. Sessa, J.V. Cross, D.J. Templeton, and K.M. Shokat. 2005. A second-site suppressor strategy for chemical genetic analysis of diverse protein kinases. *Nat. Methods*. 2:435–441. http://dx.doi.org/10.1038/nmeth764

Zhang, L., J. Li, L.H. Young, and M.J. Caplan. 2006. AMP-activated protein kinase regulates the assembly of epithelial tight junctions. *Proc. Natl. Acad. Sci. USA*. 103:17272–17277. http://dx.doi.org/10.1073/pnas.0608531103

Zheng, B., and L.C. Cantley. 2007. Regulation of epithelial tight junction assembly and disassembly by AMP-activated protein kinase. *Proc. Natl. Acad. Sci. USA*. 104:819–822. http://dx.doi.org/10.1073/pnas.0610157104